Development of Xenopus laevis bipotential gonads into testis or ovary is driven by sex-specific cell-cell interactions, proliferation rate, cell migration and deposition of extracellular matrix

Rafal P. Piprek, Malgorzata Kloc, Jean-Pierre Tassan, Jacek Z. Kubiak

Development of *Xenopus laevis* bipotential gonads into testis or ovary is driven by sex-specific cell-cell interactions, proliferation rate, cell migration and deposition of extracellular matrix

Rafal P. Piprek[*1], Malgorzata Kloc[2,3,4], Jean-Pierre Tassan[5,6] and Jacek Z. Kubiak[5,6,7]

[1]Department of Comparative Anatomy, Institute of Zoology and Biomedical Research, Jagiellonian University, Krakow, Poland
[2]The Houston Methodist Research Institute, Houston, TX, USA
[3]Department of Surgery, The Houston Methodist Hospital, Houston TX, USA
[4]University of Texas, MD Anderson Cancer Center, Houston TX, USA
[5]CNRS, UMR 6290, Institute of Genetics and Development of Rennes, Cell Cycle Group, 35043 Rennes, France
[6]Université Rennes 1, Faculty of Medicine, 35043 Rennes, France
[7]Laboratory of Regenerative Medicine and Cell Biology, Military Institute of Hygiene and Epidemiology (WIHE), Warsaw, Poland

Corresponding author:
Rafal P. Piprek
Department of Comparative Anatomy
Institute of Zoology and Biomedical Research
Jagiellonian University
Gronostajowa 9
30-387 Krakow, Poland
Phone: +48126645059
e-mail: rafal.piprek@uj.edu.pl

Abstract

Information on the mechanisms orchestrating sexual differentiation of the bipotential gonads into testes or ovaries in amphibians is limited. The aim of this study was to investigate the development of *Xenopus laevis* gonad, to identify the earliest signs of sexual differentiation, and to describe mechanisms driving these processes. We used light and electron microscopy, immunofluorescence and cell tracing. In order to identify the earliest signs of sexual differentiation the sex of each tadpole was determined using genotyping with the sex markers. Our analysis revealed a series of events participating in the gonadal development, including cell proliferation, migration, cell adhesion, stroma penetration, and basal lamina formation. We found that during the period of sexual differentiation the sites of intensive cell proliferation and migration differ between male and female gonads. In the differentiating ovaries the germ cells remain associated with the gonadal surface epithelium (cortex) and a sterile medulla forms in the ovarian centre, whereas in the differentiating testes the germ cells detach from the surface epithelium, disperse, and the cortex and medulla fuse. Cell junctions that are more abundant in the ovarian cortex possibly can favor the persistence of germ cells in the cortex. Also the stroma penetrates the female and male gonads differently. These finding indicate that the crosstalk between the stroma and the coelomic epithelium-derived cells is crucial for development of male and female gonad.

Keywords: gonad; testis; ovary; sexual differentiation; stroma; germ cells; *Xenopus*

1. Introduction

The sexual differentiation of the gonadal anlagen into testis or ovary requires a binary developmental decision. During this process a distinct testis- or ovary-specific structures emerge and the bipotential gonad acquires features enabling it to produce sperm or eggs, and male or female steroid hormones (Piprek et al., 2016). The gonad development, the formation of sex cords and the molecular and cellular mechanisms driving these processes have been described in details in mammals (Hummitzsch et al. 2013; Nel-Themaat et al., 2009; reviewed in Piprek 2016), chicken (Smith and Sinclair, 2004; Smith et al., 2007), and red-eared turtle *Trachemys scripta* (Yao et al., 2004). These studies indicated that among various developmental processes, the cell proliferation and migration are crucial for establishment of the gonadal fate (Schmahl et al., 2000; Schmahl and Capel, 2003; Tilmann and Capel, 1999). In amphibians, the development of gonads has been extensively studied at the light microscopy level (Falconi et al., 2004; Piprek et al., 2010; Saotome et al., 2010; Tanimura and Iwasawa, 1988, 1989; Witschi, 1929). The structure of developing amphibian gonads deviates from that of amniotes, and it is unknown whether the mechanisms responsible for testis and ovary development in amphibians and amniotes are similar. *Xenopus laevis* is a model anuran species, and many laboratories studied the role of steroid hormones and xenobiotics (Piprek et al., 2012 and citations there; Piprek et al., 2013a) and gene expression (Osawa et al., 2005; Piprek et al., 2013a; Yoshimoto et al., 2008) in developing gonads of *X. laevis*. However, developmental mechanisms driving sexual differentiation of *Xenopus* gonads are still poorly understood. The studies of the structural aspects of gonad development in *X. laevis* are limited to primordial germ cell migration and their settlement in the earliest genital ridges (Wylie and Heasman, 1976), the organization of germ cells during ovarian cyst formation (Kloc et al., 2004), and the induction of meiosis (Piprek et al., 2013b). Previously, we studied the external structure of developing gonads in *Xenopus* and other anurans (Piprek et al., 2014). Witschi

(1929) described the early structural changes during gonad development in *Lithobates sylvaticus*. The ultrastructure of developing gonads was studied in *Pelophylax nigromaculatus*, *Rhacophorus arboreus*, *Bufo bufo*, *Bombina variegata* (Falconi et al., 2004; Piprek et al., 2010; Tanimura and Iwasawa, 1988, 1989). Cell proliferation was studied in *P. nigromaculuarus* and *Glandirana rugosa* (Saotome et al., 2010; Tanimura and Iwasawa, 1991). Many studies were focused on the gene expression in developing gonads in *G. rugosa* because of its unusual mode of sex determination (Kato et al., 2004; Nakamura, 2009; Oike et al., 2016; Oike et al., 2017; Oshima et al., 2005; Yamamura et al., 2005).

The aim of present study was to investigate the morphology of the gonads at the earliest stages of gonads formation in *Xenopus*, and to shed a light on cellular and molecular mechanisms of gonad development and sexual differentiation in *Xenopus*. We used genotyping to establish the sex of analyzed animals before they were morphologically distinguishable, and analyzed morphology of the gonads using light and transmission electron microscopy. These analyses indicated that the early testes and ovaries differ in cell adhesion and extracellular matrix formation. In order to get further insight into mechanisms driving early gonad development we studied cell junctions and the extracellular matrix (ECM) formation, as well as cell proliferation and migration. We discuss *Xenopus* gonad development in the context of other vertebrates, and address the question if the vertebrate gonadogenesis is driven by an universal mechanism.

2. Materials and Methods

2.1. Animals

Larvae of the African clawed frog (*Xenopus laevis* Daudin, 1802; Pipidae) were obtained in the laboratory. The tadpoles were reared in 10-L aquaria (30 tadpoles per 10 L) at 22^{o}C and fed with powder food Sera Micron (Sera) daily. They were staged according to

Nieuwkoop and Faber (1956). After staging tadpoles from the stage NF45 until stage NF66 (completion of metamorphosis) were anesthetized with 0.1% MS222 solution. Numbers of analysed specimens are shown in Suppl. Table 1. All the specimens used in experiments were acquired according to Polish legal regulations concerning the scientific procedures on animals (Dz. U. nr 33, poz. 289, 2005) and the permission from the First Local Commission for Ethics in Experiments on Animals.

2.2. Gender determination by PCR

The genetic sex of tadpoles was determined using PCR detection of female-specific *DMW* gene. DNA was isolated from tadpole tails using NucleoSpin Tissue Kit (Macherey-Nagel, 740952.240C). *DMW* gene (W-linked female-specific marker) and *Dmrt1* gene (positive control) were used to determine ZZ or ZW status of tested animals. PCR was performed as previously described (Yoshimoto et al., 2008). The mixture of the following pairs of primers were used: for *DMW*: 5'-CCACACCCAGCTCATGTAAAG-3' and 5'-GGGCAGAGTCACATATACTG-3', and 5'-AACAGGAGCCCAATTCTGAG-3' and 5'-AACTGCTTGACCTCTAATGC-3' for *Dmrt1*.

2.3. Light microscopy

The tadpoles were dissected and the whole urogenital ridges (mesonephroi and gonads) were fixed in Bouin's solution overnight, dehydrated and embedded in paraffin (Paraplast, Sigma, P3683). Samples were serially sectioned at 6 μm, and stained with hematoxylin and picroaniline according to Debreuill's procedure (Kiernan, 1990). This trichromatic staining allowed for visualization of extracellular matrix, stroma, and thus gonadal interior structure. Images were taken with Nikon Eclipse E600 light microscope.

2.4. Transmisison Electron Microscopy

Urogenital ridges were dissected from tadpoles and fixed in Karnovsky's fixative. After rinsing in cacodylate buffer and postfixtion in 1% osmium tetroxide solution (Ito and Karnovsky, 1968), samples were dehydrated and embedded in Epon812. Ultra-thin sections were stained with uranyl acetate and lead citrate. The sections were analyzed using JEOL JEM2100 transmission electron microscope. The germ cells were easily distinguishable due to their big size, and large, pale, euchromatic nuclei.

2.5. Immunohistochemistry

Bouin's solution-fixed and paraffin-embedded samples were serially sectioned at 4μm. Sections were deparaffinated, rehydrated and heat-induced epitope retrieval was performed using sodium citrate buffer (10 mM sodium citrate, 0.05% Tween-20, pH 6) at 95ºC for 20 min. Subsequently, the sections were blocked with 3% H_2O_2 followed by 6% Bovine Serum Albumin (BSA, Sigma) and incubated with primary antibodies (rabbit polyclonal anti-laminin #L9393, Sigma; anti-E-cadherin #ab152102, Abcam; both 1:200) for 15 min at room temperature (RT), and with UltraVision Quanto Detection System (ThermoFisher, TL-125-QHD). Mayer's hematoxylin was used as a counterstain. Sections were viewed under Nikon Eclipse E600 microscope.

2.6. Proliferation assay

In order to investigate cell proliferation we used BrdU labeling and PCNA immunodetection. Bromodeoxyuridine (BrdU, Sigma, B5002) was diluted in PBS (10 mM; pH 7.4) and 50 μL of solution was injected intraperitoneally to the tadpoles. After 24, 48, and 72 h tadpoles were anesthetized and gonads were dissected and fixed in Bouin's solution overnight.

Bouin's solution-fixed, deparaffinised and rehydrated samples were rinsed in PBS. Samples were boiled in citrate buffer (10 mM tri-sodium citrate, 0.05% Tween-20, pH 6.0) to retrieve epitopes. Then samples were incubated with blocking solution (6% Bovine Serum Albumin (BSA, Sigma) for 30 min followed by overnight incubation with primary antibodies in PBS with 1% BSA. The primary antibodies against BrdU (1:1000, mouse monoclonal antibody, Sigma, B8434) and against human PCNA (1:3000, rabbit polyclonal antibody, Sigma, HPA030521) were used. Incubation with secondary antibodies was performed at RT for 1 h with Cy3-conjugated goat anti-mouse secondary antibodies (Sigma, C2821) at 1:100 dilution or with Alexa Fluor 488-conjugated goat-anti rabbit secondary antibodies (ThermoFisher, A20181) at 1:200 dilution. DAPI (10μM; Sigma, D9542) was used to stain nuclei. Samples were mounted with SlowFade Gold Antifade Reagent (Molecular Probes). Immunostained samples were viewed under confocal microscopy LSM 510 META.

2.7. Cell counting

For total and proliferating cell counting we used 4μm-thick sections immunostained for PCNA as described in 2.6. Analysis was performed with Nikon Eclipse E600 fluorescence microscope. Cell counting was performed on five sections through the gonomere of the medial part of the gonad, and averaged for each gonad. The cell number was counted from three gonads from the same sex and NF stage. Analyses were performed with the use of statistical software package Statistica (version 12.0 StatSoft PL).

2.8. Cell migration assay

Gonads with attached mesonephroi (entire bilateral urogenital ridges) were placed in sterile *in vitro* culture medium (L-15 33.3 mL; RPMI1640 33.3 mL; FBS 6.65 mL; water 26 mL; supplemented with L-glutamin 660 μL; penicillin 100 IU/mL; streptomycin 100μg/mL;

neomycin 200µg/mL; all products from Sigma). 100 µL of a cell tracer (a mixture of 50 mM Mitotracker and 0.5 mg/mL 5-carboxytetramethylrhodamine, succinimidyl ester from Molecular Probes) was pipetted onto each complex and incubated for 30 min. as previously described (Darnell et al., 2000; Yao et al., 2004). After washing in culture medium the urogenital ridges were placed in a tissue culture plate covered with sterile agar (1.5% in serum-free culture medium) (Martineau et al., 1997; Tilmann and Capel, 1999). After the agar solidified, 1 ml of culture medium was pipetted into the well. After 30 min. of incubation with cell tracer, samples were placed in the medium, covered and incubated in a sterile chamber at 20^{o}C for 96 h and subsequently fixed. The samples fixed immediately after incubation with the cell tracer were used as a control. The samples were fixed in 4% paraformaldehyde overnight at 4^{o}C and after washing in PBS, impregnated in sucrose (12%, 50% each for 2 hours), embedded in cryomatrix (Shandon) and immediately frozen in liquid nitrogen. Samples were cut using cryostat Leica CM 1850 UV. After staining with DAPI (10 µM; Sigma, D9542) for 30 min at RT, samples were mounted with ProLong Diamond Antifade Mountant (ThermoFisher, P36965) and viewed under confocal microscope LSM 510 META.

2.9. SDS-PAGE and Western blotting

To assess specificity of antibodies we performed sodium dodecyl sulfate polyacrylamide gel electrophoresis (SDS-PAGE), and Western blotting. Whole testes isolated from individuals at metamorphosis were homogenized in Laemmli buffer. Homogenates were subjected to electrophoresis on 8-12% SDS-PAGE gel (Laemmli, 1970). Separated proteins were transferred to nitrocellulose membranes (Hybond C, Amersham) according to standard procedures and probed with rabbit polyclonal antibodies against E-cadherin (1:3000, #ab152102, Abcam), PCNA (1:3000, HPA030521, Sigma), and anti-laminin (1:5000, #L9393, Sigma). Antigen–antibody complexes were visualized using alkaline phosphatase

conjugated anti-rabbit secondary antibody (1:20,000) in combination with Enhanced Chemifluorescence reagent (ECF; Amersham). Signal quantification was performed using ImageQuant 5.2 software (Amersham). Western blot results are presented in Suppl. Fig. 1.

3. Results and Discussion

3.1. First steps of gonadogenesis – development of undifferentiated gonads

3.1.1. Structural changes leading to the formation of genital ridges

The development of the gonad starts when the primordial germ cells (PGCs) migrate from the gut through the dorsal mesentery to the ventral surface of the vena cava (a large vein located between both mesonephroi) (Fig. 1A-C). This takes place about 9-13 days after fertilization, i.e. between NF48 and NF49 stage, when the hind limb buds appear in the tadpoles. Wylie and Heasman (1976) described the ultrastructure of migrating PGCs and their settlement in the genital ridges. During the migration through dorsal mesentery the PGCs establish contacts with the coelomic epithelium and with the extracellular matrix (ECM) located between both sheets of mesentery (Fig. 1B). Before PGCs migration into their final position, at the sites of the future gonad, the coelomic epithelium forms a typical monolayer of epithelial cells underlined by a basal lamina (Fig. 1A-C). The under-epithelial basal lamina disappears in the locations of PGCs migration. The earliest sign of gonad formation becomes noticeable when the PGCs migrate along the mesentery. At this stage two bulged genital ridges form along both sides of dorsal mesentery (Fig. 1A, C). The sites of genital ridge formation at the ventral surface of the vena cava were previously described in *X. laevis* (Wylie and Heasman, 1976) and other anurans such as *L. sylvaticus* (Witschi, 1929). While the sites of genital ridge formation are similar between different anuran species, in the amniotes, the genital ridges form at the ventromedial surface of the mesonephroi (reviewed in Piprek et al., 2016). During the formation of genital ridges, the epithelial cells, after gaining

contact with the PGCs, flatten and the basal lamina under coelomic epithelium disappears. At this stage the genital ridge forms a bulge containing PGCs (usually 1 or 2 visible in a single cross section) covered by a flattened monolayer epithelium (gonadal surface epithelium) without a basal lamina (Fig. 1D, E). Such an early step of gonadogenesis was previously described in mouse and bovine fetuses (Hu et al., 2013; Hummitzsch et al., 2013). A common feature of this early step, which represents the onset of genital ridge formation, is the disappearance of basal lamina. The second process observed in the earliest gonads of mouse and cattle was intensive proliferation of somatic cells, which transformed the genital ridge into the cluster of cells with submerged PGCs. These events are common for all amniotes (Smith and Sinclair, 2004; Smith et al., 2007; Yao et al., 2004). In contrast, in *Xenopus* and other amphibians (Piprek et al., 2010), during the early steps of gonad development there is no intensive proliferation of somatic cells (Fig. 2), and the PGCs become enclosed by a monolayer of flattened coelomic epithelial cells.

None of the previously published studies had clarified if the formation of the genital ridges in amphibians coincides with the PGCs settlement (Piprek et al., 2010; Wylie and Heasman, 1976). Our histological analysis showed that the folding of the coelomic epithelium and its transformation into the genital ridges precedes the settlement of PGCs. Fig. 1A shows the stage (NF48/49) when two small folds of coelomic epithelium had been already formed (Fig. 1A, B, C; gr) while the PGCs are still located in the dorsal mesentery. This indicates that the genital ridges form before the entry of PGCs, and shows that in *Xenopus* the PGCs do not induce genital ridge formation. This is in agreement with our previous observation that the absence of PGCs (chemically eradicated with busulfan) (Piprek et al., 2012) does not prevent formation of the genital ridges.

After settling in the genital ridge the PGCs lose yolk. From this point of time the PGCs are termed the gonial cells (Ogielska, 2009; Witschi, 1929). The gonial and somatic

cells contact through the electron-dense zones of cell membrane without any structures characteristic of desmosomes or adherens junctions, and morphologically resemble accumulations of cell adhesion molecules at the cell surface (Fig. 1E; a). In contrast, the desmosome-like junctions and tight junctions interconnect the surface epithelial cells (somatic cells) of the genital ridge (Fig. 1E; TJ and D). Tight junctions are always present near the apical part, whereas desmosome-like junctions are closer to the basal part of epithelial cells, which is a typical distribution for this type of cells (see the diagram in Fig. 1F). Such a distribution of cell junctions in gonadal surface epithelium persists throughout the whole period of gonadal development in both sexes. This confirms that the cells at the surface of developing gonad preserve an epithelial character and suggests that in amphibians the cell junctions may be crucial for gonad development. In contrast, in the early genital ridges of bovine embryo, the coelomic epithelium cells lose the epithelial features and undergo epithelial-to-mesenchymal transformation (Hummitzsch et al., 2013).

By the NF50 stage of development the gonads grow due to the increase in the number of somatic surface epithelium, which is especially visible in the proximal region (nearest to the mesonephroi) of the gonad where the gonadal mesentery starts to develop (Fig. 1G, gm, and 2). The gonadal mesentery forms two epithelial sheets underlined by a basal lamina (Fig. 1G, I). The mesentery divides the undifferentiated gonad into proximal and distal regions. The proximal region remains the gonadal mesentery, while the distal region contains germ cells covered by the surface epithelium without the basal lamina. All germ cells are attached directly to the surface epithelium via electron-dense zones of cell membrane (Fig. 1H).

3.1.2. Cell proliferation and migration – formation of the gonadal medulla

At stage NF51, the somatic cells are visible not only at the surface, but also inside the gonad (Fig. 1J). The EM analysis showed that initially all somatic cells are arranged in a

monolayer row (NF50), later some somatic cells elongate inwards the gonad and eventually lose their connection with the surface epithelium (NF51) (Fig. 1K, L; ic). This indicates that some somatic cells leave the surface epithelium and invade the interior of the gonad. In the distal region of the gonad the somatic cells enclose germ cells, while in the proximal region the somatic cells gather under the epithelium.

From the NF52 stage onwards, the number of somatic cells located inside the gonads increases (Fig. 2), and they form the group of cells between both sheets of gonadal mesentery (Fig. 1M). This is the early step of the gonadal medulla formation (Fig. 1M, m). The medulla cells are joined by desmosome-like junctions (Fig. 1N) and form a cluster. The gonadal medulla grows and a final structure of undifferentiated gonad becomes established (Fig. 1O). The medulla fills the center of the gonad and gonadal mesentery. All germ cells are located at the distal region of the gonad constituting the gonadal cortex. These are the first signs of partition into cortex and medulla (see the diagram in Fig. 1O). The gonad partition into cortex and medulla is universal for all anurans, however, the timing of the partition is species-specific (reviewed in Ogielska, 2009; Piprek et al., 2010).

We used cell-tracing assay to investigate the origin and the fate of somatic cell lines in developing gonads. We found that in *Xenopus* the coelomic epithelium transforming into somatic cells of the genital ridges expresses E-cadherin (Fig. 3). We observed that starting from stage NF51, the cells accumulating inside the gonad and all cells of the gonadal medulla are E-cadherin-positive. (Fig. 3). This strongly suggests that medulla cells originate from the gonadal surface epithelium and not from the extragonadal tissues as previously suggested (Cheng, 1932; Christensen, 1930; Lopez, 1989; Rugh, 1951; Swingle, 1926; Witschi, 1929,1956; Vannini and Sabbadin, 1954). To further prove the origin of cells inside the gonads, we performed cell migration assay. We detected cell tracer in the somatic cells of the

medulla, which indicates that these cells derive from the gonadal surface epithelium (Fig. 4A).

The analysis of cell proliferation showed that the most intensive cell divisions occur in the proximal region of the genital ridge, i.e. at the site of gonadal mesentery and medulla formation (Figs. 5A, E). Altogether, the above analyses suggest that the cells of gonadal mesentery proliferate and ingress inwards, and thus give rise to the gonadal medulla.

Previously, the precise studies of cell proliferation and cell migration in early gonad development were only performed in mouse (Capel et al., 1999; Schmahl et al., 2000; Schmahl and Capel, 2003). In mouse the surface epithelium covering the whole undifferentiated gonad proliferate. Thus, the whole gonadal surface is a source of somatic cells. In contrast, in *Xenopus*, cell proliferation is limited to the epithelium covering the proximal region adjoining mesonephros.

3.1.3. Stroma appearance in the undifferentiated gonads

By the NF52/53 stage of *Xenopus* development, the stroma appears in the undifferentiated gonad as a distinct cell line (Fig. 1Q, R). Easily recognizable in electron microscope, fibroblast-like stroma cells give rise to future connective tissue that will constitute an internal scaffold of the gonad. These cells are initially visible in the gonadal mesentery and during penetration into the gonads. Thus, these cells most likely immigrate from the mesonephroi. The stroma is negative for E-cadherin and thus can be easily distinguished from the cortex and medulla (Fig. 3). Immunolocalization, and cell tracing indicated that stroma does not originate from the surface gonadal epithelium, and thus has different origin than the cortex and medulla.

The immunolocalization of E-cadherin, which marks gonadal cortex and medulla, but not the stroma, are very useful to visualize the process of gonad formation (Fig. 3). Using

immunolocalization and trichromatic stain we visualize the stroma penetrating between the cortex and medulla, and the basal laminae forming at the interface of cortex and stroma and at the interface of medulla and stroma (Fig. 6A, 7A, 8C). The germ cells were always enclosed by the coelomic-epithelium- derived cells (pre-Sertoli and pre-follicular cells that differentiate into supporting cells), and they never contacted the stroma or the basal lamina. The developing gonads of all studied anuran species contain stroma between cortex and medulla (Falconi et al., 2004; Piprek et al., 2010; Saotome et al., 2010; reviewed in Ogielska, 2009).

Many studies suggested that stroma is important for the gonad development in the amniotes. In the mouse, cattle, chicken, and turtle the stroma penetrating developing gonads separates sex cords, and thus patterns the gonadal structure (Capel et al., 1999; Hummitzsch et al., 2013; Smith and Sinclair, 2004; Smith et al., 2007; Yao et al., 2004). This takes place at different stages in different species. In cattle, chicken and turtle the stroma separates sex cords before sexual differentiation of the gonads. In mouse, the gonads develop rapidly from the coelomic epithelium and the stroma invades gonads when they start differentiation into ovaries and testes, and thus separates ovigerous or testis cords, respectively. In *Xenopus*, as in other anurans, the stroma penetration starts in the undifferentiated gonads, however, in contrast to other amniotes, it separates cortex from medulla, but not the sex cords. Further studies are needed to identify factors regulating stroma penetration, which seems to be crucial for the establishment of the gonadal structure.

3.2. Sexual differentiation of the gonads

3.2.1. The earliest signs of sexual differentiation of the gonads

The earliest sign of sexual differentiation of *Xenopus* gonads is visible at the stage NF53 (about 23 days after fertilization) when there is a subtle difference in location of the germ cells in both sexes. In the differentiating ovaries (the gonads of *DMW*-positive

individuals, i.e. the genetic females), the germ cells retain their initial attachment to the gonadal surface epithelium and thus stay in their original, peripheral position (Fig. 6A, C, I) while the center of the gonad is occupied by a sterile medulla. In differentiating testes (the gonads of *DMW*-negative individuals, i.e. the genetic males) the germ cells lose their connections with the gonadal surface epithelium, move inwards, and disperse within the gonad (Fig. 6B, D, J). The medulla is absent because it fuses with the cortex. This sex-specific feature is decisive for the structure of future ovaries and testes.

Previous descriptions of the gonadogenesis in anurans were oversimplified (Witschi, 1929). It was claimed that the germ cells are initially located in the cortex, and translocate to the medulla in the differentiating testes (Witschi, 1956). The comparison between *Xenopus* and other vertebrates shows that there is a universal sex-specific manner of germ cell location, common for amphibians and amniotes. In many amniotes, such as turtle, chicken, swine, cattle and human, the germ cells are incorporated into the peripheral germinal epithelium in differentiating ovaries, while in differentiating testes the germ cells locate in the center of the gonad (Pelliniemi, 1975; Smith and Sinclair, 2004; Smith et al., 2007; Yao et al., 2004). Interestingly, the mouse deviates from this pattern. In the mouse there is no clear partition into the cortex and medulla and all germ cells are dispersed throughout the gonad (reviewed in Piprek et al., 2016).

3.2.2. Sex-specific pattern of cell proliferation and migration

After identification of the earliest sign of sexual differentiation, we searched for cellular mechanisms responsible for establishment of the ovarian or testis structure. We noticed three aspects of gonadogenesis that seem to be crucial for sexual differentiation of *Xenopus* gonad.

First, we found sex-specific changes in the pattern of cell proliferation and migration. In the differentiating ovaries, the most intensive cell divisions are detectable in the proximal region of the gonad, i.e. in the gonadal mesentery and medulla. This indicates that cell proliferation sites are similar for undifferentiated gonad and differentiating ovaries (Fig. 5B, F). Cell migration assay showed that in the undifferentiated gonads and ovaries cells from the gonadal surface accumulate in the gonadal medulla and also occasionally in the cortex (Fig. 4D, E). In contrast, in differentiating testes the proliferating cells are scattered within the whole surface of the gonad and especially in its distal part (Fig. 5C, G). Cells ingressing from the gonadal surface eventually disperse within the whole developing testes (Fig. 4B, C). The program of development of undifferentiated gonad and ovarian development seems to be similar, while the differentiation into testis requires distinct developmental switch.

Besides finding the sex-specific differences in distribution of proliferating and migrating cells during sexual differentiation of gonads in *Xenopus*, we additionally found that the number of somatic and germ cells increases gradually during gonad development (Fig. 2). This increase was highest in the testes from the onset of sexual differentiation. A rapid intensive cell proliferation of coelomic epithelium covering the gonad was described as a first sign of testis differentiation in the mouse (Schmahl et al., 2000; Schmahl and Capel, 2003). As a result, one day after the onset of sexual differentiation, the developing mouse testis becomes two times bigger than the ovary. In *G. rugosa* there is no significant difference in somatic cell number between testes and ovaries at the early phase of sexual differentiation (Saotome et al., 2010). Thus, it is not clear if a cell number increase in testis differentiation is a common mechanism for all vertebrates.

3.2.3. Contribution of the cell junctions to sexual differentiation

We observed sex-specific changes in distribution of the cell junctions during sexual differentiation of *Xenopus* gonads (Suppl. Fig. 2). Numerous well-developed desmosome-like junctions are present between somatic cells in the ovarian cortex, while in the developing testes the cell junctions are undetectable (Fig. 6E). This implies that in the differentiating ovaries the adhesion of germ cells to the gonadal surface epithelium may be responsible for the germ cell persistence in the original cortical position. In contrast, in differentiating testes the cell adhesion seems to be significantly weaker. The lack of strong adhesion may be responsible for the dispersion of germ cells within the male gonad (Fig. 6F). Thus, we postulate that the cell adhesion between the somatic cells enclosing germ cells may be of great importance for the location of germ cells. Dispersion of germ cells in the differentiating testes may not be a result of their active migration; but may be caused by the displacement of the germ cells by proliferating somatic cells at the gonadal surface.

There is no information on the cell junctions during gonadal development in other vertebrates. Our study, for the first time, indicates that the cell junctions are involved in sexual differentiation of the gonads. Further experiments should prove if cell junctions play decisive role in the establishment of testis versus ovary structure.

3.2.4. The role of the stroma in sex-specific structure patterning during sexual differentiation of the gonads

We found that developing ovaries and testes in *Xenopus* differ in the pattern of stroma penetration. In differentiating ovaries the stroma forms continuous wide layer separating peripheral cortex from the cluster of medulla cells (Fig. 6G). Thus, the ovary has clearly separated cortex and medulla (see the scheme at Fig. 6I). because in the ovary the germ cells remain attached to the gonadal surface epithelium they are present exclusively in the cortex, whereas the medulla is sterile. In contrast, in differentiating testes, many branches of stroma

irregularly penetrate the gonad interior (Fig. 6D, H; and diagram in Fig. 6J) and the cortex and medulla fuse. As a result, the germ cells, detached from epithelium, spread within the whole gonad, and the surface epithelium of differentiating testis becomes sterile and underlined with stroma. Also the structure of stroma differs in developing gonads of both sexes. In the tadpole ovaries the stroma is loose and contains many loosely dispersed collagen fibers. In the tadpole testes the stroma does not have visible collagen fibers, and, in EM images, has a form of dark and amorphous ribbons of ECM components (Fig. 6C, D). This indicates a sex-specific behavior of the stromal cells.

It had been suggested that the stroma plays a crucial role in sexual differentiation of mouse gonads (Capel et al., 1999). In developing mouse testes the streams of mesonephros-derived stromal cells pattern the formation and distribution of testis cords. In differentiating mouse ovaries, the stroma is much less abundant, but also penetrates the interior of the gonad and separates ovigerous cords. The stroma was also described in developing bovine gonads (Hummitzsch et al., 2013). In cattle, similarly to many other amniotes, starting from the beginning of the development, the stroma separates sex cords in undifferentiated gonads (Pelliniemi, 1975; Smith and Sinclair, 2004; Yao et al., 2004). During sexual differentiation of mouse gonad the stroma separates the centrally located sex cords into seminiferous tubules in the testes and the peripheral cords into ovarian follicles in the ovaries. In amphibians, gonadal stroma contribution to sexual differentiation of the gonad is apparently different. First, no sex cords are formed in the undifferentiated gonads, but rather one layer of stroma separates cortex from medulla. Such separation of cortex and medulla by a sheet of stroma is typical for all studied anurans, but is absent in amniotes (Hummitzsch et al., 2013; reviewed in Ogielska, 2009; Witschi, 1929; Yao et al., 2004). Thus, the structure of amphibian ovary visibly deviates from that in the amniotes. However, both in developing amphibians and amniotes the stroma separates cords and underlines sterile surface epithelium.

3.3. Development of the ovary

By the NF55 stage (about 35 days after fertilization), all individuals have gonads already sexually differentiated, and both ovaries and testes are morphologically distinguishable. In the earliest ovaries, the stroma is well differentiated and is separated from the cortex and medulla by two basal laminae (Fig. 7A, arrows). All oogonia (female gonial cells) are located in the peripheral (cortical) position, and are attached to the surface epithelium. At the NF56 stage, the primary oogonia start divisions with incomplete cytokineses forming a cyst of secondary oogonia connected by intercellular bridges (Fig. 7B). The ovarian cyst is covered by an envelope of flattened somatic (pre-follicular) cells connected to the ovarian surface epithelium (Fig. 7C). Somatic cells are joined by the desmosome-like cell junctions (Fig. 7C, arrowheads).

At the NF57 stage, the secondary oogonia in the ovarian cysts enter meiosis (Fig. 7D). Oocytes in leptotene, zygotene and pachytene stages are still connected by cytoplasmic bridges, however, in the late pachytene the follicular cells penetrate between the oocytes and the cysts break down into the ovarian follicles (within each follicle a single oocyte is enclosed by a monolayer of flattened follicular epithelium). By comparison, in mouse the oocytes are separated later, i.e. in the diplotene (Pepling and Spradling, 2001). Thus, among vertebrates, the cyst breakdown may occur at slightly different stages.

At stage NF58, the oocytes enter diplotene and some of them start intensive growth (Fig. 7E), the ovarian follicles move towards the center of the ovary and become enveloped by stroma (Fig. 7F). The stroma along with basal laminae also squeezes into the cortex and thus separates the ovarian cysts and follicles (Fig. 7G). This suggests another role of the stroma in gonad development – it not only shapes the structure of the ovary but also participates in the breakdown of the ovarian cysts into ovarian follicles. In amphibians and

amniotes, the folliculogenesis occurs in a similar manner. Follicular cells and stroma penetrate between oocytes, and germ cells cysts disintegrate. The first follicles form in the central region of the ovary and this process proceeds towards ovarian periphery. In amphibians, some of the primary oogonia remain under surface epithelium as a reservoir for oogenesis in the next reproductive seasons.

Along with the rearrangement of the ovarian cortex the structural changes take place in the ovary interior. Here the medulla (a cluster of somatic cells joined by desmosome-like junctions) is enclosed by the basal lamina that separates it from the stroma (Fig. 6A, E, G; m, arrows). Soon after the onset of ovarian differentiation at NF53 stage, the medullary cells lose cell junctions and delaminate, which results in the formation of the intramedullary lumen (secondary ovarian cavity) (Figs. 6A, 7J). The medullary cells polarize and desmosomes locate at their lateral sides (Fig. 7J). The basal regions of medulla cells contact basal lamina and their apical regions face the ovarian cavity (Fig. 7H). As a result, the medulla transforms into a typical simple epithelium lining the ovarian cavity and covering the ovarian follicles (Fig. 7H). The internodal region of the ovary does not have cavity and the center of the internodal region is filled by stroma (Figs. 3F, 7D; see 3.5).

By the NF58 stage (Fig. 7E), when all medullary cells are already transformed into epithelial cells and the secondary cavity fills the center of developing ovary, the ovarian follicles squeeze towards the ovarian cavity, while the epithelium of the cavity and a thin sheet of the stroma cover the ovarian follicles. As a result, each diplotene oocyte is surrounded by monolayer of follicular cells, basal lamina (derived from the basal lamina of the cortex), stroma, basal lamina (derived from the basal lamina of the medulla), and epithelium of the ovarian cavity (Fig. 7F, H, Supp. Fig. 2D). The presence of basal laminae enclosing the ovarian follicles was observed in all studied anurans (e.g. Falconi et al., 2004; reviewed in Ogielska and Bartmanska, 2009; Piprek et al., 2010; Saotome et al., 2010).

During ovarian development there is a decrease in proliferation of somatic and germ cells (Fig. 2B). The decrease in the number of proliferating germ cells after the onset of meiosis was also described in *G. rugosa* (Saotome et al., 2010).

The comparison between *Xenopus* and other amphibians indicates that in all amphibians the development of the ovaries follows a common pattern with slight differences resulting from various rates of development (reviewed in Ogielska and Bartmanska, 2009; Ogielska and Kotusz, 2004). However, the ovary structure in amphibians differs from the one in amniotes. In amphibians, the ovaries do not have sex cords and consist of two distinct parts: cortex and medulla with ovarian cavity. In the ovaries the medulla is always sterile (lacks the germ cells) and it transforms into the simple epithelium lining the ovarian cavity. Such a secondary cavity is present only in amphibians (Ogielska and Bartmanska, 2009). A cavity appears also in the ovaries of teleost fishes, however, ovarian cavity in both groups are not homologous; in fishes the ovarian cavity forms as a result of gonad folding and fusion, rather than the formation of space inside the gonad as in amphibians (Liu et al., 2010; Pandian, 2012). In the amniotes, many streams of stroma penetrate whole differentiating ovaries and separate ovigerous cords (Hummitzsch et al., 2013; Pelliniemi, 1975; Smith and Sinclair, 2004; Yao et al., 2004). Germ cells are located peripherally, and the cords located centrally remain sterile and constitute the ovarian medulla. Thus, the peripheral location of germ cells and the presence of sterile tissue in the ovary center is a common feature. Peripheral location of germ cells presumably relates to the fact that oocytes are released from the ovarian surface. The presence of secondary cavity in the ovary is unique to amphibians, and may be related to the production of giant size oocytes that locate near the cavity. We noticed that the ovarian cavity shrinks with the increase in the oocyte size.

3.4. Development of the testis

By stage NF55, all testes are easily distinguishable due to the lack of the diversification into the cortex and medulla, and the dispersion of germ cells within the whole gonad (Fig. 8A, B). In EM images, the testes are easily recognizable by many irregularly positioned branches of the stroma (Fig. 6D). The branches of the stroma shape the interior structure of developing testes, establishing the location of the compartment containing spermatogonia (male gonial cells) enclosed by somatic cells (pre-Sertoli cells). These compartments become surrounded by the basal laminae separating them from the stroma, and form the testis cords (Figs. 6F, H, 8F). The process of testis cord formation is depicted in a series of images in Fig. 8B-F. The fully developed testis cords are visible at NF60 stage. Unlike in ovary, the stroma is present around each testis cord in the form of narrow sheet of dark, amorphous mass of ECM components. The presence of the basal laminae around forming anuran testis cords was also shown by EM in *B. bufo* (Falconi et al., 2004), *B. variegata* (Piprek et al., 2010), and by immunolocalization of laminin in *G. rugosa* (Saotome et al., 2010).

While the proliferating cells in developing testes are dispersed within the whole gonad, they are the most abundant in the distal region (Fig. 5C, G). In contrast, in the ovaries the most intensive proliferation occurs in the proximal region. We also observed an intensive proliferation in the surface epithelium covering the developing testis (Fig. 5C, G). This proliferation coincided with an ingression of cells from the gonadal surface (Fig. 4B). The ingression ceases around stage NF60, i.e. when the testis cords had been already formed and stroma separates sterile surface epithelium (Fig. 4C). After the NF60 stage, cell proliferation continues within the testis cords (Fig. 2). This indicates that intensive cell proliferation and ingression provide a supply of cells during the early phase of testis development. Interestingly, in mice, the proliferation and ingression of coelomic epithelium, which contribute cells to the testis cords, are restricted to the narrow time-window (between 11.2

and 11.4 days after coitum) and later the cells from the gonadal surface do not contribute to the testis cords formation (Karl and Capel, 1998; Schmahl et al., 2000). Cell proliferation in developing testes was also studied in other anurans. Tanimura and Iwasawa (1991) described high proliferation in the region that differentiates into the testis cords. Saotome et al. (2010) reported the proliferating cells dispersed in the testis cords of developing male gonads in *G. rugosa*. Our study, showed how the changes in the pattern of cell proliferation and migration contribute to the formation of the testis structure.

It seems that in vertebrates the development of testis structure occurs through a common mechanism. In all studied amniotes and anurans the stroma ingressing from the mesonephros separates testis cords and patterns the gonad (Karl and Capel, 1998; Pelliniemi, 1975; Smith and Sinclair, 2004; Yao et al., 2004). The differences in this process are the result of various development rates between different species. In amphibians, including *X. laevis*, *L. sylvaticus*, *G. rugosa*, and in mice, the cords arise late, after the onset of sexual differentiation of the gonads (Saotome et al., 2010; Witschi, 1929). However, in amniotes with slower rate of development, such as chicken, swine or cattle, the phase of undifferentiated gonads is longer and the stroma invades the undifferentiated gonads, and thus sex cords form at this early stage (Hummitzsch et al., 2013; Pelliniemi, 1975; Smith and Sinclair, 2004; Yao et al., 2004). During sexual differentiation, the sex cords become ovarian or tesis cords. In the mouse, the streams of migrating cells from the mesonephros are responsible for patterning the testis cords (Capel et al., 1999). Disruption of this cell migration impairs testis cord formation. In all studied vertebrates, during testis differentiation the germ cells locate in the gonadal centre, and the epithelium covering the testis becomes sterile, unlike in the ovaries. Also in all studied species, the male germ cells are enclosed in elongated cords giving rise to tubules or lobules in which spermatogenesis takes place. These

spermatogenic structures join the mesonephric tubules through which the sperm will exit the gonads.

3.5. Structural changes in the gonads during sexual differentiation visualized in the longitudinal sections

Several novel aspects of gonadogenesis in *Xenopus* were revealed during histological analysis of the longitudinal sections. In the genital ridges the somatic cells are dispersed (Fig. 9A); however, from NF52 the medulla cells gather into about 14 groups located along the long axis of the gonad, and the cortex and medulla become easily distinguishable (Fig. 9B). Along with the growth of the medulla the gonomeres with nodal and internodal regions become clearly visible in external morphology of the gonad (Piprek et al., 2014). During the ovarian differentiation this metamerism becomes more distinct due to the appearance of separate secondary cavity in each gonomere. As a result the gonad consists of a row of beads (Fig. 9C, D). Such a structure of developing gonads is typical for Archaeobatrachia (more basal groups of anurans), however, gonadal metamerism is absent in Neobatrachia, such as Hylidae, Bufonidae and Ranidae (Piprek et al., 2014).

Serial cross sections through the gonads at the site of the node (Fig. 7B) or internodal region show structural differences (Fig. 7D). Within each node, the sterile medulla is in the centre, and the stroma forms a layer around the medulla. In the internodal region, the medulla is absent and the stroma fills the centre of the gonad.

In differentiating testes, due to the fusion of the cortex and medulla, the nodes (gonomeres) are lost and the testes acquire an even surface and a spindle shape (Fig. 9E, F). Nevertheless, in the centre of the testis persists a small cluster of medulla cells (Fig. 8E). These cells will give rise to the rete testis (data not shown).

4. Conclusions and future perspectives

In summary, our analyses indicate a series of mechanisms driving gonad development and determining the testis or ovary structure formation in *Xenopus*. Different location of proliferating and migrating cells, diverse distribution of cell junctions, and different penetration by stroma are probably crucial for sexual differentiation of the gonads.

We indicated that there are several cellular processes common for gonadogenesis in amphibians and amniotes, nevertheless, we also pointed out a series of differences between these groups. Yoshimoto et al. (2008) described the genetic of sex determination in *X. laevis*; *DMW* is a sex-determining gene triggering female sex differentiation. Here, we described the earliest signs and cellular processes driving sexual differentiation. However, further studies are necessary to establish what genes and factors regulate cell proliferation and migration during amphibian gonad development, and how the cell interactions, assembly and disintegration of the cell junctions control cell gathering, stroma ingrowth and the basal lamina deposition. Further studies are also necessary to show how the sex determination genes (*DMW* and *Dmrt1*) control the realization of the female or male program of gonad formation.

Acknowledgements

The study was conducted within the project financed by the National Science Centre assigned on the basis of the decision number DEC-2013/11/D/NZ3/00184.

References

Capel, B., Albrecht, K.H., Washburn, L.L., Eicher, E.M., 1999. Migration of mesonephric cells into the mammalian gonad depends on *Sry*. Mech. Dev. 84, 127–31.

Cheng, T.H., 1932. The germ cell history of *Rana cantabrigensis* (Baird): I. Germ cell origin and gonadal formation. Z. Zellfrosch. Mikrosk. Anat. 16, 497–541.

Christensen, K., 1930. Sex differentiation and development of oviducts in *Rana pipiens*. Am. J. Anat. 45, 159–187.

Darnell, D.K., Garcia-Martinez, V., Lopez-Sanchez, C., Yuan, S., Schoenwolf, G.C., 2000. Dynamic labeling techniques for fate mapping, testing cell commitment, and following living cells in avian embryos. Methods Mol. Biol. 135, 305–321.

Falconi, R., Dalpiaz, D., Zaccanti, F., 2004. Ultrastructural aspects of gonadal morphogenesis in *Bufo bufo* (Amphibia Anura) 1. Sex differentiation. J. Exp. Zool. A 301, 378–388.

Hu, Y.C., Okumura, L.M., Page, D.C., 2013. Gata4 is required for formation of the genital ridge in mice. PLoS Genet. 9(7):e1003629.

Hummitzsch, K., Irving-Rodgers, H.F., Hatzirodos, N. et al., 2013. A new model of development of the mammalian ovary and follicles. PLoS ONE 8(2), e55578.

Ito, S., Karnowsky, M.J., 1968. Formaldehyde glutaraldehyde fixatives containing trinitro compounds. J. Cell. Biol. 36, 168.

Karl, J., Capel, B., 1998. Sertoli cells of the mouse testis originate from the coelomic epithelium. Dev. Biol. 203, 323–333.

Kato, T., Matsui, K., Takase, M., Kobayashi, M., Nakamura, M., 2004. Expression of P450 aromatase protein in developing and in sex-reversed gonads of the XX/XY type of the frog Rana rugosa. Gen. Comp. Endocrinol. 137, 227–36.

Kiernan, J.A., 1990. Histological and Histochemical Methods: Theory and Practice. 2nd ed, Pergamon Press, Oxford, New York, Seoul, Tokyo.

Kloc, M., Bilinski, Sz., Dougherty, M.T., Brey, E.M., Etkin, L.D., 2004. Formation, architecture and polarity of female germline cyst in *Xenopus*. Dev. Biol. 266, 43–61.

Laemmli, U.K., 1970. Cleavage of structural proteins during the assembly of the head of bacteriophage T4. Nature 227, 680–685.

Liu, Z.H., Zhang, Y.G., Wang, D.S., 2010. Studies on feminization, sex determination, and differentiation of the Southern catfish, *Silurus meridionalis* – a review. Fish Physiol. Biochem. 36, 223–235.

Lopez, K., 1989. Sex differentiation and early gonadal development in *Bombina orientalis* (Anura: Discoglossidae). J. Morphol. 199, 299–311.

Martineau, J., Nordqvist, K., Tilmann, C., Lovell-Badge, R., Capel, B., 1997. Male-specific cell migration into the developing gonad. Curr. Biol. 7, 958–968.

Nakamura, M., 2009. Sex determination in amphibians. Semin. Cell Dev. Biol. 20, 271–82.

Nel-Themaat, L., Vadakkan, T.J., Wang, Y. et al., 2009. Morphometric analysis of testis cord formation in Sox9-EGFP mice. Dev. Dyn. 238, 1100–1110.

Nieuwkoop, P.D., Faber, J., 1956. Normal tables of *Xenopus laevis* (Daudin). 1st ed Amsterdam, North-Holland.

Ogielska, M., Kotusz, A., 2004. Pattern of rate of ovary differentiation with reference to somatic development in anuran amphibians. J. Morphol. 259, 41–54.

Ogielska, M., 2009. Undifferentiated amphibian gonad. In: M. Ogielska, ed., Reproduction of Amphibians, Science Publishers, Enfield, pp. 1–33.

Ogielska, M., Bartmanska, J., 2009. Oogenesis and Female Reproductive System in Amphibia-Anura. In: M. Ogielska, ed., Reproduction of Amphibians, Science Publishers, Enfield, pp. 153–272.

Oike, A., Kodama, M., Nakamura, Y., Nakamura, M., 2016. A threshold dosage of testosterone for female-to-male sex reversal in *Rana rugosa* frogs. J. Exp. Zool. A. Ecol. Genet. Physiol. 325, 532–538.

Oike, A., Kodama, M., Yasumasu, S., Yamamoto, T., Nakamura, Y., Ito, E., Nakamura, M., 2017. Participation of androgen and its receptor in sex determination of an amphibian species. PLoS One. 12:e0178067.

Osawa, N., Oshima, Y., Nakamura, N., 2005. Molecular cloning of Dmrt1 and its expression in the gonad of *Xenopus*. Zoolog. Sci. 22, 681–687.

Oshima, Y., Hayashi, T., Tokunaga, S., Nakamura, M., 2005. Wnt4 expression in the differentiating gonad of the frog *Rana rugosa*. Zoolog. Sci. 22, 689–693.

Pandian, T.J., 2012. Differentiation in Gonochores. In: T.J. Pandian, ed., Genetic Sex Differentiation in Fish, Science Publishers, USA, pp. 17–87.

Pelliniemi, L.J., 1975. Ultrastructure of gonadal ridge in male and female pig embryos. Anat. Embryol. 147, 19–34.

Pepling, M.E., Spradling A.C., 2001 Mouse ovarian germ cell cysts undergo programmed breakdown to form primordial follicles. Dev. Biol. 234, 339–351.

Piprek, R.P., Pecio, A., Szymura, J.M., 2010. Differentiation and development of gonads in the yellow bellied toad, *Bombina variegata* L. 1758 (Amphibia: Anura: Bombinatoridae). Zool. Sci. 27, 47–55.

Piprek, R.P., Pecio A, Kubiak J.Z., Szymura J.M., 2012. Differential effects of busulfan on gonadal development in five divergent anuran species. Reprod. Toxicol. 34, 393–401.

Piprek, R.P., Pecio, A., Laskowska-Kaszub, K., Kubiak, J.Z., Szymura, J.M., 2013a. Sexual dimorphism of AMH, DMRT1, RSPO1 localization in the developing gonads of six anuran species. Int. J. Dev. Biol. 57, 871–875.

Piprek, R.P., Pecio, A., Laskowska-Kaszub, K., Kloc, M., Kubiak, J.Z., Szymura, J.M., 2013b. Retinoic acid homeostasis regulates meiotic entry in developing anuran gonads and in Bidder's organ through Raldh2 and Cyp16b1 proteins. Mech. Dev. 130, 613–627.

Piprek, R.P., Pecio, A., Kloc, M., Kubiak, J.Z., Szymura, J.M., 2014. Evolutionary trend for metamery reduction and gonad shortening in Anurans revealed by comparison of gonad development. Int. J. Dev. Biol. 58, 929–934.

Piprek, R.P., 2016. Molecular Mechanisms of Cell Differentiation in Gonad Development. Springer International Publishing, Switzerland.

Rugh, R., 1951. The Frog: Its Reproduction and Development. McGraw-Hill, New York.

Saotome, K., Isomura, T., Seki, T., Nakamura, Y., Nakamura, M., 2010. Structural changes in gonadal basement membranes during sex differentiation in the frog *Rana rugosa*. J. Exp. Zool. 313A, 369–380.

Schmahl, J., Capel, B., 2003. Cell proliferation is necessary for the determination of male fate in the gonad. Dev. Biol. 258, 264–276.

Schmahl, J., Eicher, E.M., Washburn, L.L., Capel, B., 2000. *Sry* induces cell proliferation in the mouse gonad. Development 127, 65–73.

Smith, C.A., Sinclair, A.H., 2004. Sex determination: insights from the chicken. Bioessays 26, 120–32.

Smith, C.A., Roeszler, K.N., Hudson, Q.J., Sinclair, A.H., 2007. Avian sex determination: what, when and where? Cytogenet. Genome Res. 117, 165–73.

Swingle, W.W., 1926. The germ cells of anurans. II. An embryological study of sex differentiation in *Rana catesbeiana*. J. Morphol. 41, 441–546.

Tanimura, A., Iwasawa, H., 1988. Ultrastructural observations on the origin and differentiation of somatic cells during gonadal development in the frog *Rana nigromaculata*. Dev. Growth Differ. 30, 681–691.

Tanimura, A., Iwasawa, H., 1989. Origin of somatic cells and histogenesis in the primordial gonad of the Japanese tree frog *Rhacophorus arboreus*. Anat. Embryol. 180, 165–173.

Tanimura, A., Iwasawa, H., 1991. Proliferative activity of somatic cells during gonadal development in the Japanese pond frog, *Rana nigromaculata*. J. Exp. Zool. A 259, 365–370.

Tilmann, C., Capel, B., 1999. Mesonephric cell migration induces testis cord formation and Sertoli cell differentiation in the mammalian gonad. Development 126, 2883–2890.

Vannini, E., Sabbadin, A., 1954. The relation of the interregnal blastema to the origin of the somatic tissue of the gonad in frog tadpoles. J. Embryol. Exp. Morph. 2, 275–289.

Witschi, E., 1929. Studies on sex differentiation and determination in amphibians: I. Development and sexual differentiation of the gonads of *Rana sylvatica*. J. Exp. Zool. 52, 235–265.

Witschi, E., 1956. Development of Vertebrates. WB Sauders, Philadelphia.

Wylie, C.C., Heasman, J., 1976. The formation of the gonadal ridge in *Xenopus laevis*. I. A light and transmission electron microscope study. J. Embryol. Exp. Morphol. 35, 125–38.

Yamamura, Y., Aoyama, S., Oshima, Y., Kato, T., Osawa, N., Nakamura, M., 2005. Molecular cloning and expression in gonad of *Rana rugosa* WT1 and Fgf9. Zoolog Sci. 22, 1045–1050.

Yao, H.H., DiNapoli, L., Capel, B., 2004. Cellular mechanisms of sex determination in the red-eared slider turtle, *Trachemys scripta*. Mech. Dev. 121, 1393–1401.

Yoshimoto, S., Okada, E., Umemoto, H., Tamura, K., Uno, Y., Nishida-Umehara, C., Matsuda, Y., Takamatsu, N., Shiba, T., Ito, M., 2008. W-linked DM-domain gene, DM-W, participates in primary ovary development in *Xenopus laevis*. Proc. Natl. Acad. Sci. USA 105, 2469–2474.

Figure legends

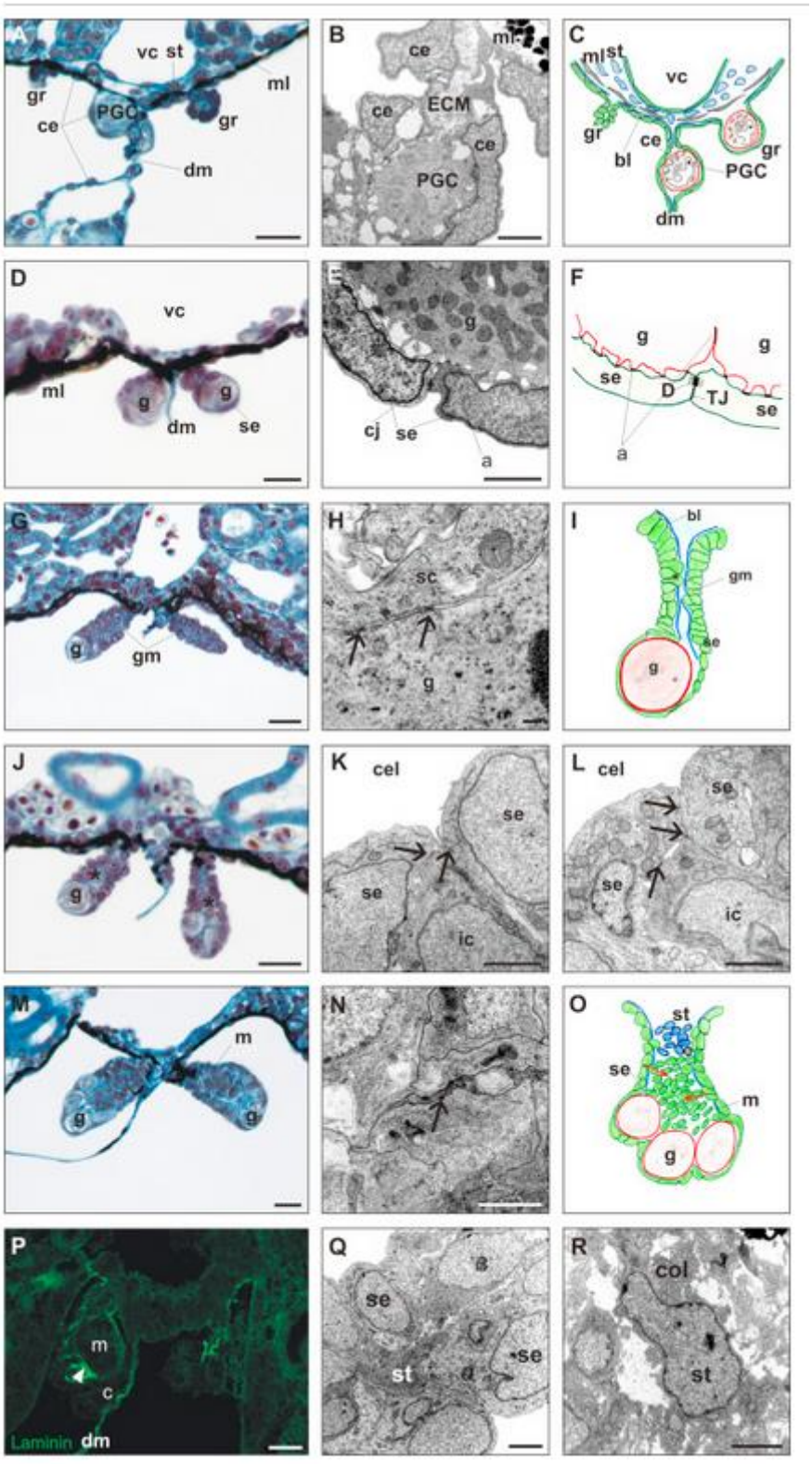

Fig. 1. The structure of undifferentiated gonad in *Xenopus laevis*.

A. The beginning of the formation of genital ridges (gr) located on both sides of the dorsal mesentery (dm), just under vena cava (vc) at NF48. Primordial germ cells (PGC) during migration through dorsal mesentery towards the genital ridges. Stroma (st) and melanophores (ml) fill the space between vena cava and coelomic epithelium (ce). The genital ridges have a form of folded coelomic epithelium.

B. Primordial germ cell (PGC) during migration through both sheets of dorsal mesentery formed by coelomic epithelium (ce). PGC adheres to the extracellular matrix (ECM) and coelomic epithelial cells without specialized cell junctions.

C. Scheme of the genital ridge (left gr) before PGC settlement, the genital ridge with PGC (right gr), and PGC during migration through dorsal mesentery. Basal lamina (bl, blue line) disappears under coelomic epithelium in the sites of genital ridge formation.

D. Undifferentiated gonads at NF49 are composed of flattened coelomic epithelial cells (gonadal surface epithelium, se) that cover germ cells (g).

E, F. EM image and diagram of the germ cells adhering to the gonadal surface epithelium (se). Germ cells form microvilli adhering (a) to the somatic cells without specialized cell junctions. Cell junctions (cj) exist between adjacent somatic cells (tight junctions, TJ, and desmosome-like junctions, D).

G. Undifferentiated gonads at NF50. Gonadal mesentery (gm) forms a proximal region of the gonad, and the germ cells are located in the distal region. First cells ingressing from the gonadal surface epithelium inwards the gonads are visible (asterisk).

H. EM image of adjacent somatic (sc) and germ cell (g) at NF50. Both cells adhere to each other by electron dense points (arrows); basal lamina is absent.

I. Diagram of undifferentiated gonads at NF50. The gonad has a form of monolayer epithelium enclosing germ cell (g) in the distal region; basal lamina (bl) is absent in the sites of contact with germ cell and ingressed somatic cells (asterisk).

J. Undifferentiated gonads at NF51. Increase of the number of somatic and germ cells, and accumulation of somatic cells in the gonadal center (between both sheets of the gonad mesentery) (asterisk).

K, L. EM images of ingression of cells from the gonadal surface epithelium toward the gonad center. Changes in the location of cell junctions are visible. **K**. Ingressing cell (ic) is the one of the gonadal surface epithelial cells (se); all cells are joined by cell junctions (arrows). **L**. Two surface epithelial cells (se) joined to each other above the ingressing cell (ic) which losses its connection with coelomic cavity (cel). Cell junctions (arrows).

M. Undifferentiated gonads at NF52. In the center of the gonads the medulla forms a mass of somatic cells. Such undifferentiated gonads are composed of the cortex and medulla (m). All germ cells (g) are located exclusively at the periphery and are all joined to the gonadal surface epithelium.

N. EM image of medulla cells forming a cluster of tightly packed cells joined by desmosome-like junctions.

O. Diagram of undifferentiated gonads at NF52. Arrows indicate direction of cell ingression from the surface epithelium (se).

P. Immunofluorescence of laminin reveals deposition of basal lamina (arrowhead) between the cortex (c) and medulla (m) in the undifferentiated gonads at NF52.

Q. EM image of stromal cell (st) present between both sheets of surface epithelium in gonadal mesentery at NF52.

R. EM image of stromal cell (st) in the undifferentiated gonad at NF53. The stromal cell is surrounded by abundant extracellular matrix containing mainly collagen fibers (col). Scale bars: A,D,G,J,M,P 20 μm; B,E 5 μm; K,L,N,Q,R 2 μm; H 200 nm.

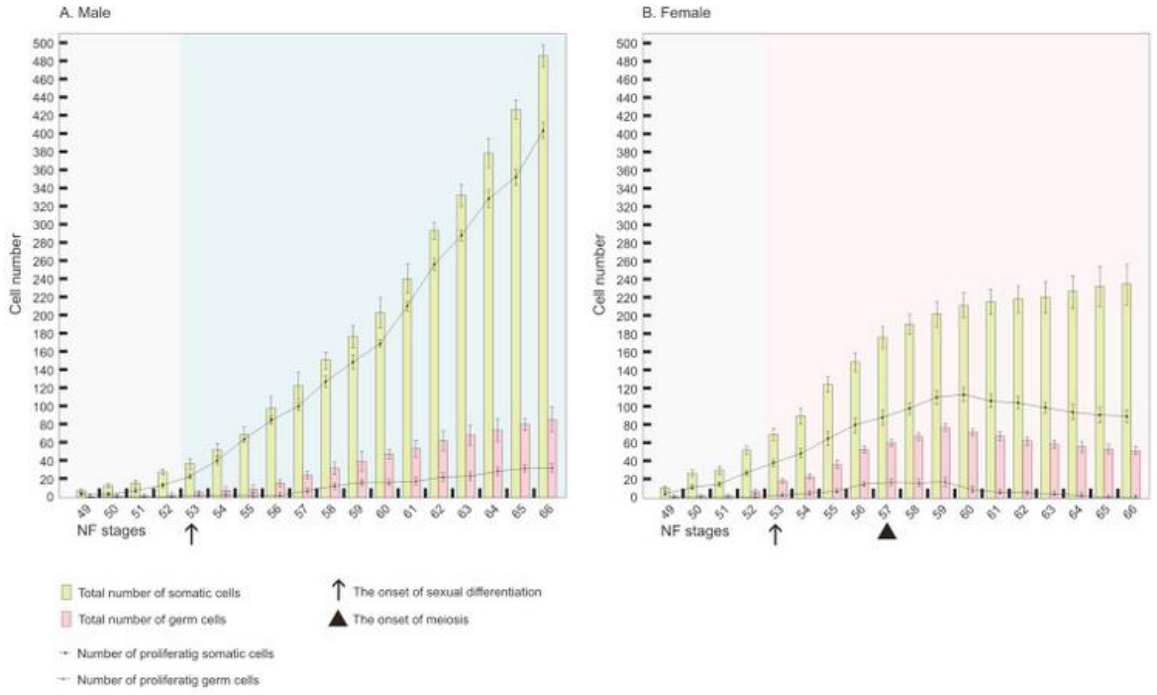

Fig. 2. Changes in the somatic and germ cell number during development of testes (A) and ovaries (B).

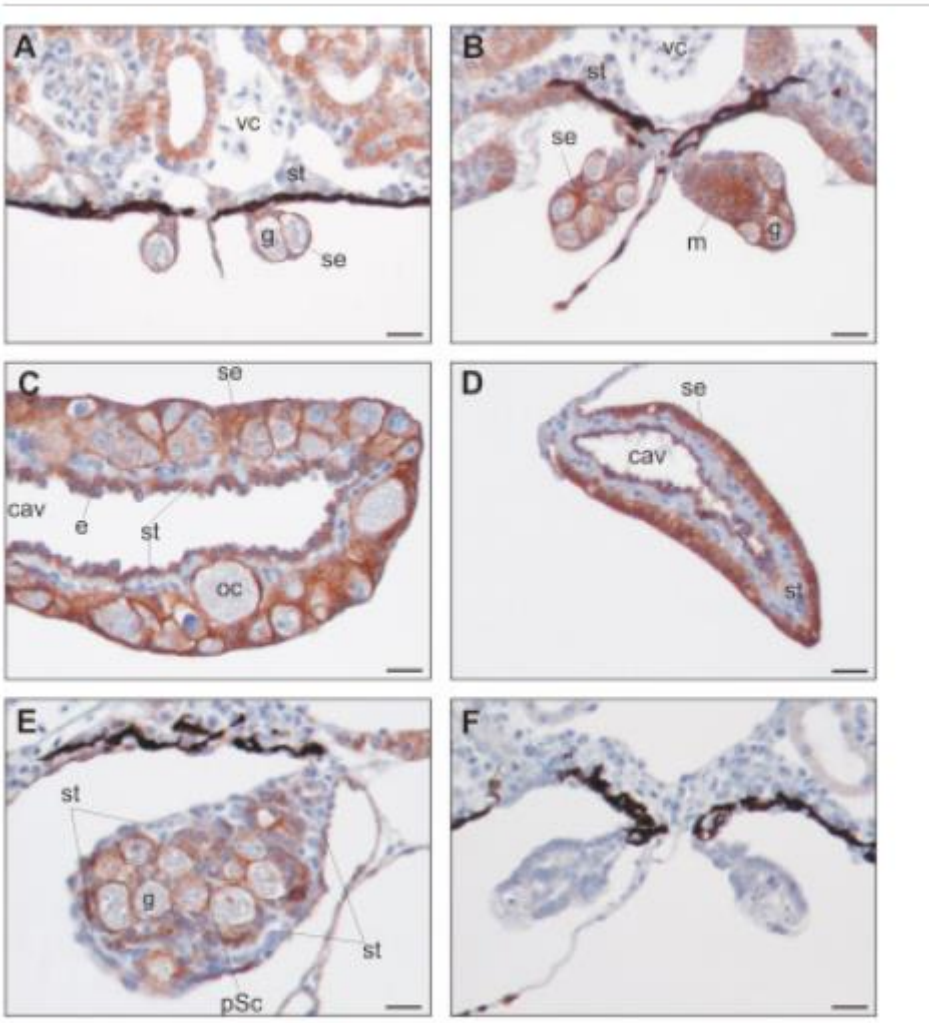

Fig. 3. Immunolocalization of E-cadherin marks somatic cells derived from coelomic epithelium. **A**. Undifferentiated gonads at NT49; E-cadherin is present in surface epithelium (se) but not in stromal cells (st). **B**. Undifferentiated gonads at NF52; E-cadherin is present in the gonadal surface epithelium (se) and medulla (m) but not in stroma (st). **C**. The ovary at NF58; E-cadherin is present in cortex and epithelium (e) lining ovarian secondary cavity (cav) originating from the medulla, E-cadherin is absent in the stroma (st). **D**. Sterile ovary at NF58 clearly shows that surface epithelium (se) and epithelium lining ovarian secondary cavity are positive for E-cadherin (indicating common origin), and stroma (st) is E-cadherin negative. **E**. Testes at NF57; E-cadherin is present mainly in the somatic cells enclosing spermatogonia (pre-Sertoli cells, pSc), lower E-cadherin signal is present in surface epithelium, and there is

no E-cadherin in the stroma (st). **F**. Negative control; undifferentiated gonads at NF52. Scale bar 20 μm.

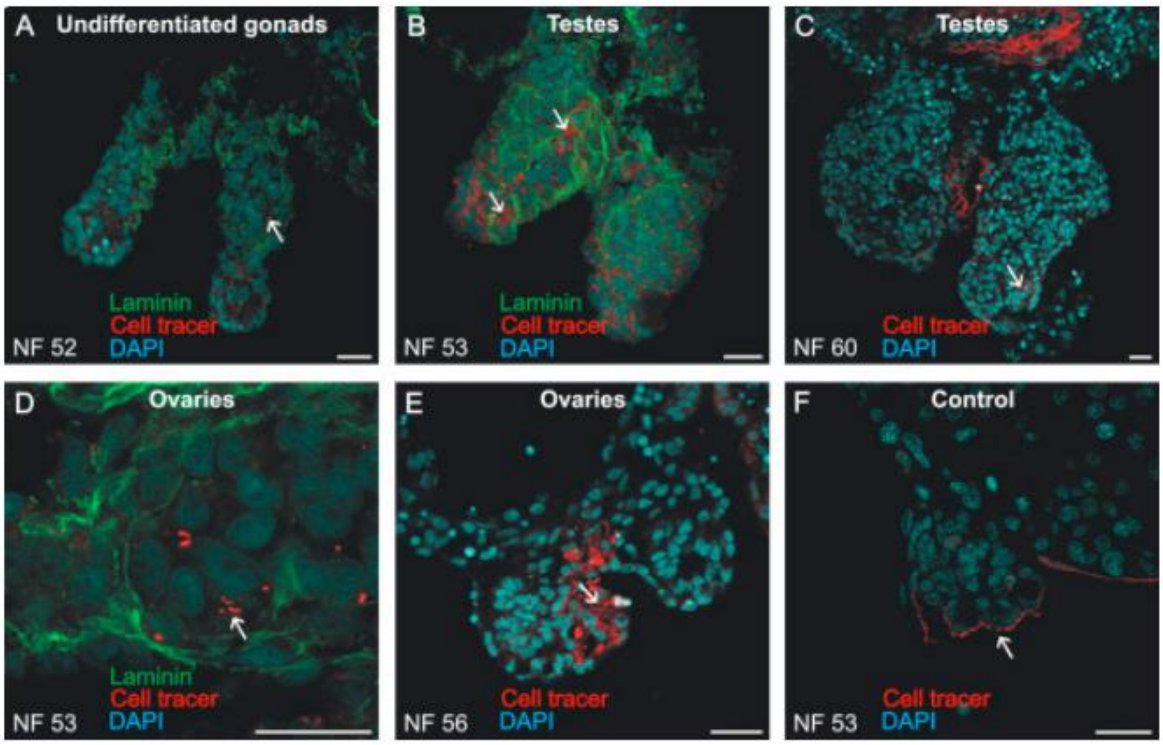

Fig. 4. Cell tracing during gonad development. A. Undifferentiated gonads at NF52; signal is visible in cells located inside the gonads, which indicates the ingression of cells from the surface epithelium inwards the gonads. **B**. Testes at NF53; signal is visible in cells dispersed in the whole gonads. **C**. Testes at NF60; only low signal is present at the gonadal surface. **D**. Ovaries at NF53; signal is present in the cells located inside the gonads. **E**. Ovaries at NF56; signal is present inside the gonads. **F**. Control gonads at NF53; signal is present only at the gonadal surface. Scale bar 60 μm.

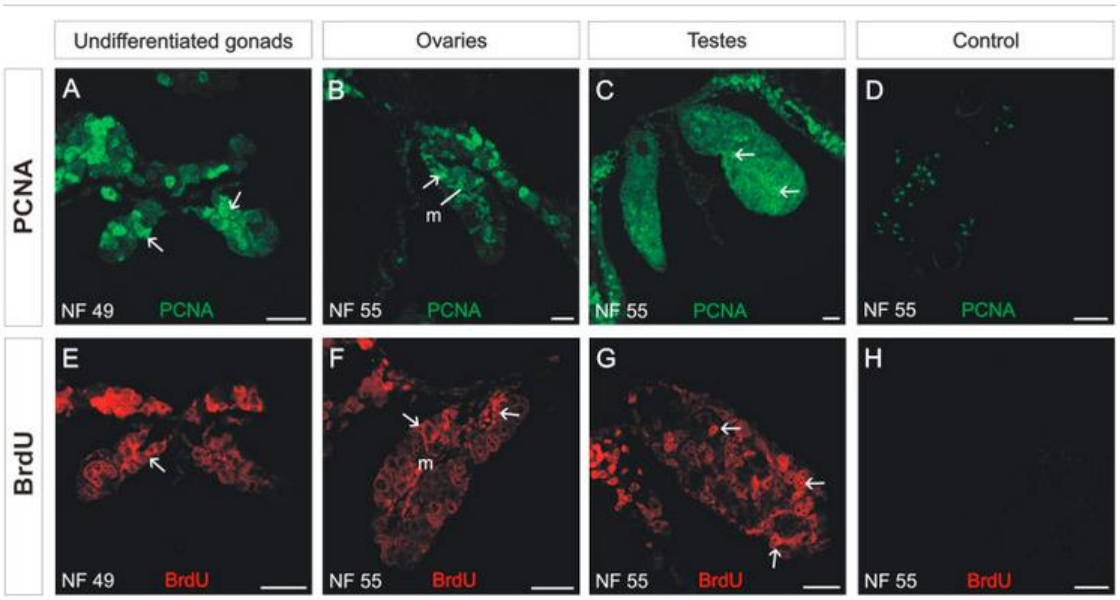

Fig. 5. Cell proliferation during gonad development assessed by PCNA (A-D) and BrdU (E-H) immunolocalization. A, E. Undifferentiated gonads at NF51; the most intensive signal is visible in the proximal part of the gonads (forming gonadal mesentery, arrows). **B, F.** Ovaries at NF55; the most intensive signal is visible in the proximal part of the gonads (ovarian mesentery), and in the gonadal medulla (m). **C, G.** Testes at NF55; proliferating cells are dispersed throughout gonads. **D, H.** Negative control at NF55. Scale bar 60 μm.

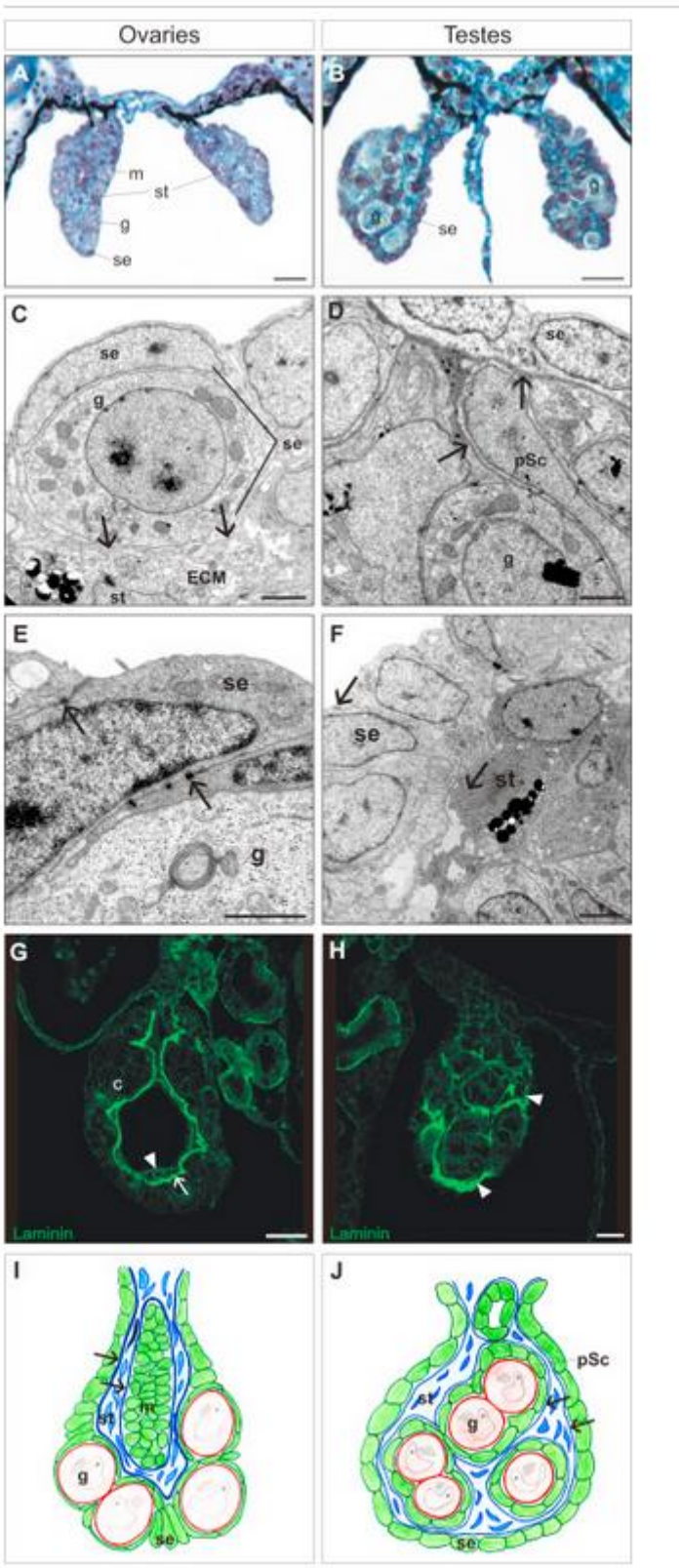

Fig. 6. Changes in gonad structure during sexual differentiation. A. The earliest signs of ovarian differentiation at NF53; Left panel shows the ovary composed of cortex, and medulla (m) with cavity (ovarian secondary cavity); stroma (st) is located between cortex and medulla;

all oogonia (g) are attached to the surface epithelium (se); Right panel shows the cross section of the ovary through its internodal region; the medulla is absent and stroma fills the center of the gonad; scale 20 μm. **B**. The earliest signs of testis differentiation at NF53; there is no division into cortex and medulla; spermatogonia (g) detach from surface epithelium and disperse within whole gonads; scale 20 μm. **C**. EM image of ovarian cortex at NF54; oogonium (g) is directly attached to the surface epithelial cell (se) and completely enclosed by it; basal lamina is present (arrows) under the somatic cell (se) and separate the cortex from underlying stroma where stromal cells (st) are surrounded by extracellular matrix (ECM). **D**. EM image of testis surface at NF54; spermatogonium (g) is enclosed by pre-Sertoli cell (pSc) and does not contact surface epithelium (se); thin sheets of extracellular matric (arrows) separate somatic cells and underlie sterile surface epithelium. **E**. Numerous desmosome-like cell junctions (arrows) are present between somatic cells of the ovarian cortex; there are no cell junctions between somatic and germ cell. **F**. In developing testis, cell junctions (arrows) are limited only to surface region; stromal cell (st) is easily distinguishable due to dark cytoplasm. **G**. Immunolocalization of laminin in developing ovary, indicating location of two basal laminae: under cortex (arrow) and around medulla (arrowhead). **H**. Immunolocalization of laminin in developing testis, indicating location of many branches of basal laminae (arrowheads) dispersed in the gonad and located also under thin surface epithelium. **I**. Scheme of early ovary; ingressing stroma locates between the cortex (containing oogonia) and sterile medulla (m), two basal laminae (arrows) separate stroma (st) from the cortex and medulla; all germ cells are connected to surface epithelium. **J**. Scheme of early testis; ingressing stroma separates spermatogonia and somatic cells (pre-Sertoli cells, pSc) from sterile surface epithelium. Scale bars: A,B,G,H 20 μm; C-F 2 μm.

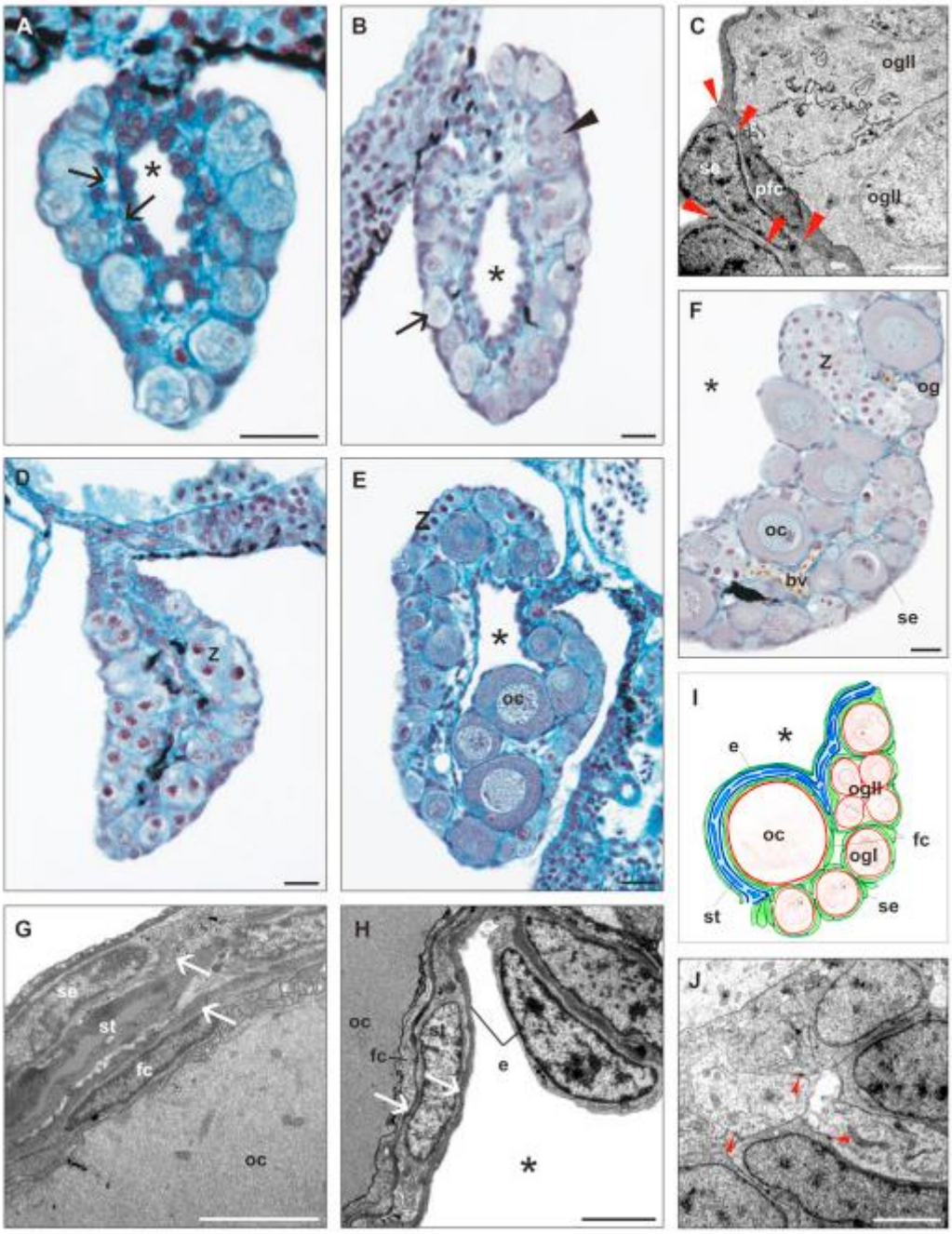

Fig. 7. Structure of developing ovaries. A. Early ovary at NF55; all oogonia (og) are attached to the surface epithelium in the ovarian cortex, cells of the ovarian medulla transform into monolayer epithelium lining the secondary ovarian cavity (asterisk); 2 basal laminae (arrows) separate stroma from the cortex and medulla. **B**. Developing ovary at NF56; in the thickening cortex. The primary oogonia (arrow) enclosed individually by somatic cells and ovarian cysts containing groups of secondary oogonia (arrowhead) are present. **C**. EM image

of ovarian cyst containing secondary oogonia (ogII) surrounded by flattened pre-follicular cells (pfc) in contact with surface epithelium (se); arrowheads indicate numerous cell junctions between somatic cells. **D**. First meiotic cells (zygotene stage, Z) are present in the ovary at NF57 (cross section through internodal region – no medulla or cavity is present); melanophores (black cells) are present in the stroma. **E**. First diplotene oocytes (oc) appear at NF58 near the ovarian cavity (asterisk). **F**. Thick ovarian cortex contains numerous germ cells; all oogonia (og) are present just under surface epithelium (se), diplotene oocytes are located near the ovarian cavity (asterisk), cysts containing zygotene oocytes are located in the middle; blood vessels (bv) and melanophores (black cells) are scattered between ovarian cysts. **G**. EM image showing surface layers of the ovary: surface epithelium (se), basal lamina (arrow), stroma (st), basal lamina (arrow), follicular cells (fc), diplotene oocyte (oc). **H**. EM image of layers enclosing diplotene oocyte (oc): follicular cell (fc), basal lamina (arrow), stroma (st), basal lamina (arrow), epithelium (e) lining ovarian cavity (asterisk). **I**. Scheme of the ovarian wall. Scale bars: A,B,D-F 20 μm; C,G-J 3 μm.

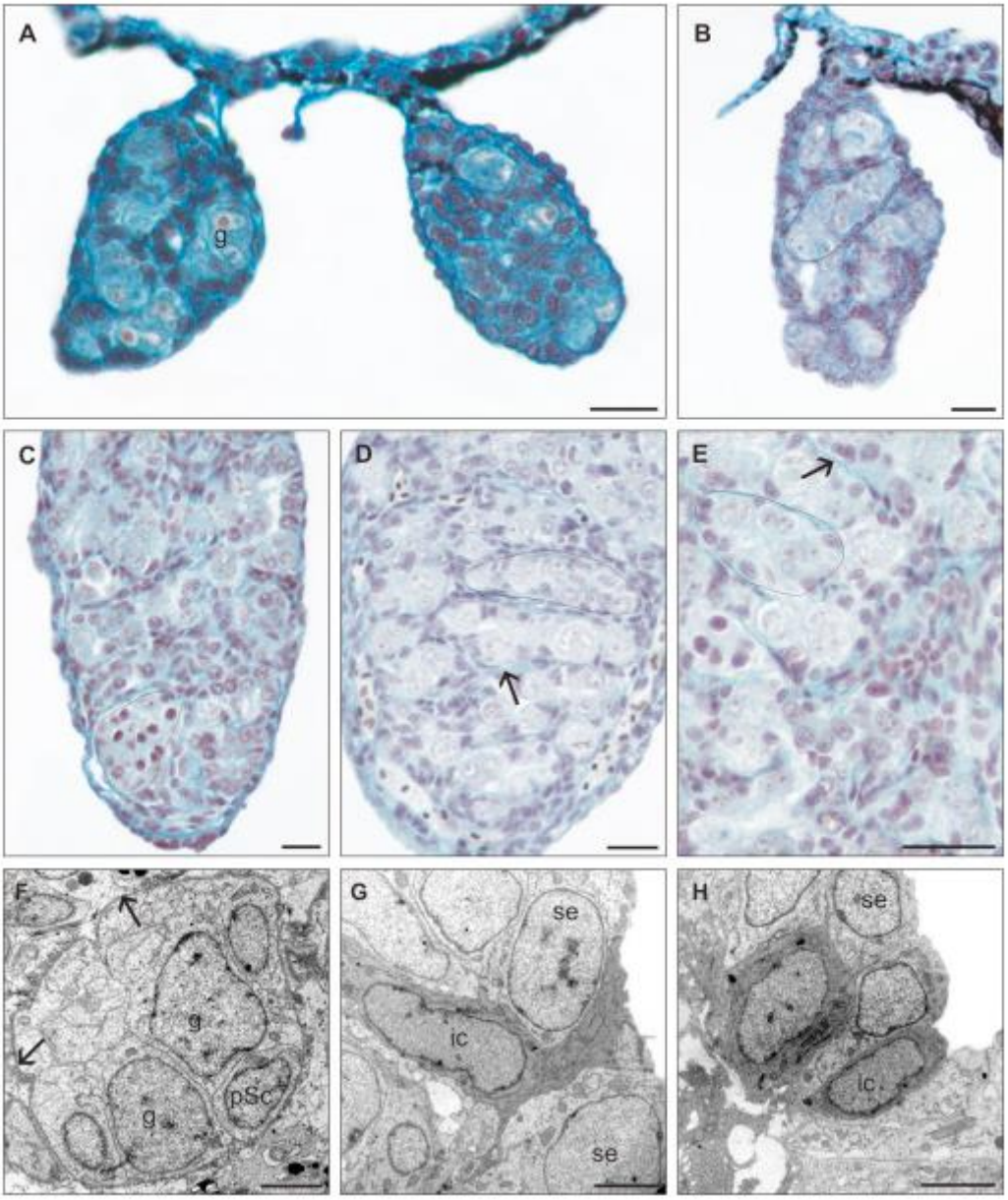

Fig. 8. Structure of developing testes. A. Early testes at NF55; all spermatogonia (g) are dispersed among somatic cells with small, dark nuclei, and do not contact surface epithelium. **B**. First signs of groups of spermatogonia (outlined) are discernible at NF56. **C**. Formation of the testis cords at NF58. **D**, **E**. The testis cords (outlined) during completion of metamorphosis (NF66); each cord becomes enclosed by basal lamina (arrow); a small cluster of somatic cells that will give rise to the rete testis is visible in the testis center. **F**. EM image of testis cord; spermatogonia (g) and pre-Sertoli cells (pSc) are enclosed by basal lamina

(arrow). **G**, **H**. Dark cells ingress (ic) inside the gonad from the superifical epithelium (se) at NF56. Scale bars: A-E 20 μm; F-H 3 μm.

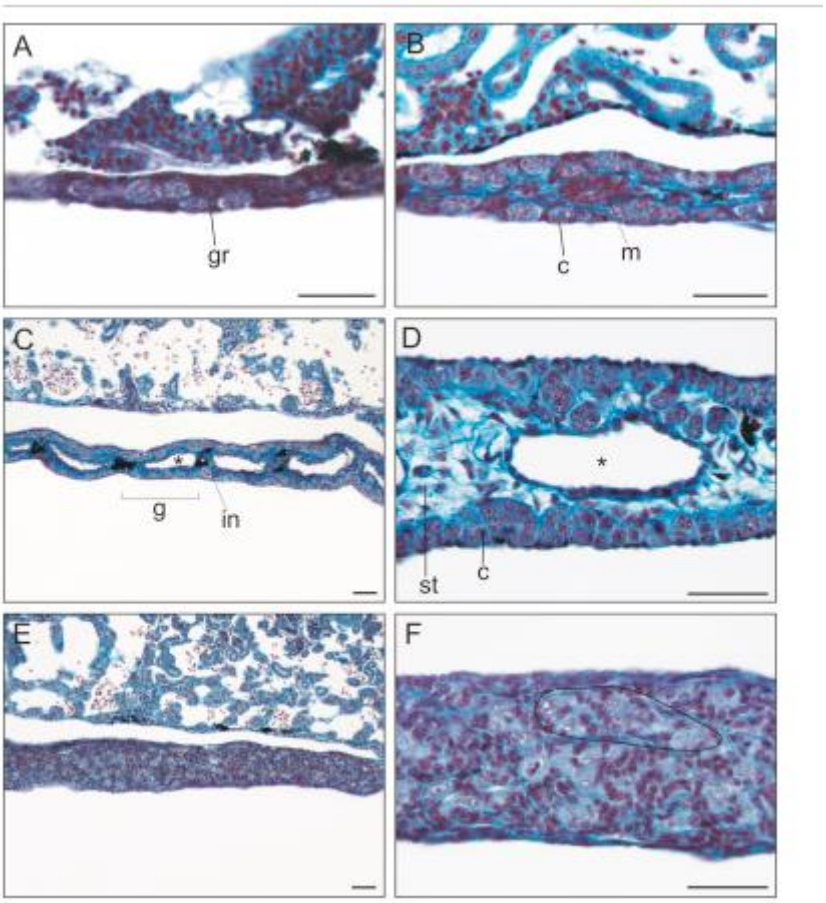

Fig. 9. Structure of developing gonads in longitudinal sections. A. Longitudinal section through the undifferentiated gonad (gr, genital ridge) at NF51. **B**. Longitudinal section through the undifferentiated gonads at NF52; cluster of medulla cells (m) and cortex (c) located peripherally are visible. **C, D**. Longitudinal section of the ovary at NG59; gonad is composed of gonomeres (g) divided by internodal regions (in) containing stroma (st), in each gonomere a secondary ovarian cavity is visible (asterisk), cortex (c) is present throughout the gonad. **E, F**. Longitudinal section of testis at NG59; there is no division into gonomeres, cortex and medulla is present, forming testis cords (rimmed) are visible in the gonads. Scale bar 50 μm.